Heat flux assessment of a solar lime multi-stage calciner operating in a CSP for thermal storage

Pilar Lisbona[a], Manuel Bailera[a], Thomas Hills[b], Mark Sceats [b], Luis I. Díez[a], and Luis M. Romeo[a]

[a] Escuela de Ingeniería y Arquitectura, Universidad de Zaragoza, Zaragoza, Spain, pilarlm@unizar.es
[b] Calix Europe (UK) Limited, Salisbury, United Kingdom.

Abstract:

Calcium-looping systems can be coupled with concentrated solar power plants as an alternative for thermal energy storage. This storage concept is based in the high temperature reversible calcination-carbonation reactions, in which limestone and lime are alternatively converted. These reactions produce or consume a specific amount of CO_2 and consume or release important quantities of thermal energy. Energy from CSP can be stored by limestone calcination (endothermic reaction) at high temperatures producing pure streams of CaO and CO_2. This energy can be later released when demand increases by means of carbonation reaction (exothermic) at relatively high temperatures. In order to produce power, the energy released in the carbonation reaction has to be transferred to a Rankine cycle. Calciner reactor is a complex system where heterogeneous chemical reactions take place while absorbing heat from a solar concentrating equipment. It is a key element of the process. Depending on the design and distribution of heat along the calciner, the amount of heat required in this reactor to store the same amount of chemical energy in the form of lime varies and the temperature of the solids strongly varies. Optimal design and operating conditions will minimize average temperature in the calciner for a given flow of produced lime. In this work, the modelling of a multi-stage solar calciner is described in the frame of a new solar-based CSP plant. The reactor will consist in a number of downward entrained flow design reactors, and the model encompasses fluid dynamics, chemical kinetics and energy balance. The results, provided along a 1-D discretization, comprise conversion rates, gas temperatures and flow rates, and heat transfer rates.

Keywords:

Ca-looping, Thermal Storage, Solar Calciner, Concentrated Solar Power.

1. Introduction

Increasing rates of electricity generation by variable renewable sources require the deployment of efficient technologies for energy storage. The integration of these storage systems is necessary to match the renewable energy availability with the electricity demand. There are several alternatives to get these buffer systems, and thermal storage seems to be the most suitable for large-scale thermoelectric power plants.

As concerns concentrated solar power (CSP) plants, energy storage enables to overcome the strong variability related to the solar energy, even in a daily basis. These storage systems are designed to operate at medium to high temperature levels, in order to achieve good values for round-trip efficiency. Heat storage by molten salts is already used in commercial power plants [1], and other alternatives as mineral oils and ceramic materials have been investigated [2].

More recently, thermochemical energy storage (TCES) has also been proposed to be integrated in concentrated solar power plants. Thermal energy is stored and released in the form of endothermic/exothermic chemical reactions, with the advantage of large energy densities in comparison to other possibilities. Several reactions have been suggested for TCES [3], being the use of $CaCO_3$/CaO one of the most promising due to its energy density (around 3.2 GJ/m^3), the large availability of limestones along with their low price.

The application of the calcium-looping (Ca-L) process has been modelled and experimented for a range of unit scales aimed to CO_2 capture [4]–[6], based on the reversible CaO carbonation / $CaCO_3$ calcination reactions (R.1).

$$CaCO_3 \leftrightarrow CaO + CO_2 \qquad \text{(R.1)}$$

A similar concept can be also conceived for concentrated solar power plants to storage energy [7], [8]. Solar energy can be used to produce the limestone calcination at high temperature (endothermic reaction), releasing and storing lime and CO_2. This chemical energy stored as lime can be used when required to release heat by the lime carbonation with CO_2 (exothermic reaction), at lower temperature –but still high enough– than the calcination one. The temperature, near to 900 °C (equilibrium temperature under a given CO_2 partial pressure of 1 atm) fits in the desirable range of high temperatures potentially attainable in CSP tower plants. This relevant feature would allow for a more efficient generation of electricity from stored energy, thus overcoming the current limitation of temperature imposed by the degradation of molten salts employed in commercial CSP plants [9], [10]. Power can be then produced by a Rankine cycle or other thermal engines with higher efficiencies [7], [8]. According to these references, good efficiencies can be achieved using Rankine cycles (35.5 %), combined cycles (39 %) or closed Joule-Brayton cycles (42 %).

To actually get these numbers, important challenges arise as concerns the design and operation modes of the reactors involved, calciner and carbonator. Constrains related to the specifics of the solar energy availability and the overall processes integration (calciner/ storage/ carbonation/ power) have to be accounted for, leading to different conditions to those modelled and tested for CO_2 capture systems.

In this paper, the modelling of a calciner in a CSP plant is addressed and the results discussed. Despite several works have been previously reported the modelling of calciner reactors for CO_2 capture by Ca-L [11], [12], the approach is here different since the heat source for limestone calcination is the solar energy. The system proposed is a multi-stage solar calciner. The target is to determine the operating conditions aiming at optimizing the efficiency and average sorption capacity, by discussing the influence of temperature distribution, as well as solar heat flow provided in each block.

2. Calcium-looping as energy storage technology

When applied as energy storage technology, the Ca-L process starts with the decomposition of $CaCO_3$ in the calcination reactor (endothermic process) producing CaO and CO_2. The high energy input required to increase the temperature of inlet streams up to the value required for the calcination reaction to occur at a sufficiently fast rate, which is essentially determined by the CO_2 equilibirum [13]. CaO and CO_2 streams are stored at ambient temperature for their use afterwards as a function of demand once sensible heat is recovered. Storage of the products could be prolonged to weeks or even months as depending on storage conditions and energy demand [14]. The reactants are recirculated into a carbonator reactor where chemical energy is released through the carbonation

reaction when energy is demanded. One of the most significant advantages of the CSP–CaL integration is the use of natural limestone as CaO precursor. Limestone is an abundant, non-toxic and cheap material (6-10 €/t), which presents suitable physical properties in the temperature range of interst for CSP thermal energy storage.

CaO from cyclic limestone calcination shows a strong deactivation under CaL specific conditions for CO_2 capture. These conditions involve high calcination temperatures under high CO_2 partial pressure [5]. It is usually assumed that this decay of CaO conversion will also limit the efficiency of the CaL process for TCES [15]. However, the cyclic conversion of CaO under calcination/carbonation conditions that optimize the efficiency of the CSP–CaL integration are different from those required for CO_2 capture and could be kept at a stable and high value. This has been confirmed by a recent thermogravimetric analysis study [16]. Thus, the lower calcination temperature, the more limited sintering in the CaO and the higher efficiency of the CaL process. Temperature of calcination will strongly depend on the distribution of heat along the calciner reactor which is the key issue to consider in this work.

To achieve similar conversion output in the calciner, different layouts of heat distributions may be applied along the calciner reactor. Better heat distributions which control temperature along the reactor in the proper values range lead to less sintering in the lime particles, faster reactions (lower dimensions required) and minimize energy consumption in this element. Thus, it is possible to improve/maximize the efficiency of the thermochemical heat storage element.

2.1. Calciner

The calciner reactor is assumed to be a solar co-current entrained flow reactor which provides heat to the endothermal calcination reaction. The calciner studied in this work presents cylindrical geometry with an initial height of 9 meters, 43 millimetres of internal diameter and 48 mm outside diameter made of stainless steel. The base case for the feed flowrate of stored $CaCO_3$ into the calciner is 5 kg/h and the gaseous atmosphere in the calciner is considered to be 100% CO_2. Pressure is considered to be constant along the calciner and equals to 1 bar. These values are related to the ongoing European SOCRATCES project (H2020 - Grant Agreement No 727348).

The distribution of heat required in a calciner is not uniform since it will depend on the temperature inside the reactor and the extent of the calcination reaction. Solar calciner design commonly provides a uniform flow of heat per length unit along the reactor which cannot be controlled. Thus, they are designed as short reactors (around 1.5-2.0 meters) with constant heat inputs in order to control the temperature of the solid inside depending on the calcination conversion. An assessment of the distribution of the heat flow is a key issue to evaluate these variables.

3. Methodology

The calciner model takes geometry, heat transfer and calcination kinetics into account, thus obtaining the temperature profiles along the carbonator under isothermal and non-isothermal conditions. The steady-state model has been implemented in EES (Engineering Equation Solver). Figure 1 illustrates the discretization scheme of the calciner model.

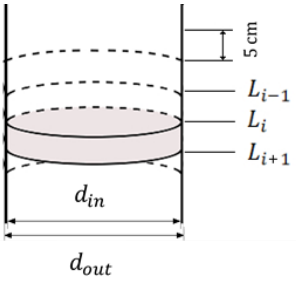

Figure 1. Discretization scheme of the calciner model.

To calculate the residence time of the gas in the carbonator, 1D plug flow is considered. The entraining velocity in downflow for the solid is calculated through the terminal velocity and the gas velocity. The reactor has been discretized in slides of 5 cm length.

3.1. Calcination kinetic model

The Generalised Random Pore Model (GRPM) has been developed by Calix. It combines the random pore models of Bhatia & Perlmutter and Gavalas [17], [18] with the shrinking core model described by Borgwardt [19], accounting for overlap through the statistics of pore intersections [20]. In this approach, the reaction front velocity r is the same for reaction in the pores and from the surface. As such, it is no longer necessary to select on or the other model depending on particle size and porosity, and sorbents which experience significant extents of calcination through both mechanisms can be more accurately modelled. The GRPM has been implemented in the calciner model. The evolution of the conversion, $X(t)$, with the residence time of the solid will follow the expression provided in (1).

$$X(t) = \int_0^t r\frac{6\cdot\left(d_p 2rt\right)^2}{d_p^3}dt + \left(1 - e^{\left(-S_{A0}rt - \pi L_{A0}(rt)^2\right)}\right)\int_t^{d_p/2k} r\frac{6\cdot\left(d_p 2rt\right)^2}{d_p^3}dt \quad (1)$$

where S_{A0} is the pore surface area calculated as the difference between BET surface area and geometrical surface area and L_{A0} is the mean pore length. A mean particle diameter d_p of 60 microns was used.

In the GRP kinetic model, the calcination reaction rate, r [m/s], is the fitting parameter of conversion calculation through (1) to the experimental data. The reaction rate is given by (2) when the atmosphere in the calciner is pure CO_2 [21].

$$r = k_o \cdot e^{\left(-\frac{E_a}{\Re T}\right)} \cdot (1-\theta_{CO2})^{N_v} \cdot \left(1 - \frac{P_{CO2}}{P_{CO2,eq}}\right) \quad (2)$$

where $k_o$is the pre-exponential factor, E_a is the activation energy, N_v is considered to take the value of 1 for limestone and θ_{CO2} is based on the Langmuir isotherm, defined through (3) where the saturation pressure is taken to be the equilibrium pressure.

$$\theta_{CO2} = \frac{\frac{P_{CO2}}{P_{CO2,eq}}}{\left(1 + \frac{P_{CO2}}{P_{CO2,eq}}\right)} \quad (3)$$

The kinetic model allows for computing the conversion of each component as a function of time, *t*. Therefore, to characterize the mass flows of different components, it is required to know the temperature, the residence time of solid and the gas in the reactor. The GRP calcination kinetic model has been implemented in the EES overall model of the multi-stage solar calciner whose results are presented in this manuscript.

3.2 Residence time for the solids

The time of interaction between the solid and the gas is limited to the residence time of the solid in the calciner since its terminal velocity must be also accounted. For those flows with Reynolds lower than 2 and small size particles, the following (4) may be applied for the downward velocity of single particles, v_s, (concentration of particles is assumed diluted) [22]:

$$v_s = v_{s,i} \cdot e^{-bt_s} + \left(v_g + v_t\right) \cdot \left(1 - e^{-bt_s}\right) \quad (4)$$

where $v_{s,i}$ is the initial velocity of the solid, v_g is the velocity of the gas phase, and v_t is the terminal settling velocity of the particle in a static fluid. The parameter b, and the velocity v_t are given by (5) and (6):

$$b = \frac{18\mu}{\rho_s d_p^2} \tag{5}$$

$$v_t = \frac{(\rho_s + \rho_g) d_p^2 g}{18\mu} \tag{6}$$

where μ is the viscosity of the gas, ρ_s is the density of the solid, ρ_g is the density of the gas, d_p is the diameter of the solid particles, and g the gravity.

The integration of (4) provides the relationship between the calciner length and the residence time of the solids (7).

$$L = \int_0^{t_{s,L}} v_s dt_s = \frac{v_{s,i}}{b}(1 - e^{-bt_s}) + (v_g + v_t) \cdot \left(t_s - \frac{1 - e^{-bt_s}}{b}\right) \tag{7}$$

It can be assumed that v_g and μ are constants in the interval of integration for the case of study. Moreover, the variation of v_t with time (due to the variation of ρ_g) can also be neglected when integrating, since $v_g \gg v_t$.

Thus, this can be directly solved by the EES software to compute the residence time of the solid as a function of the length, what will allow determining the mole flows along the reactor as a function of the distance from the entrance.

3.3 Plug flow model (1D) for the gas

The residence time of the gas is given by (8):

$$t_g = \int_0^{V_c} \frac{\pi r_{in}^2}{\dot{V}} dL \tag{8}$$

where r_{in} is the inner radius of the calciner, $\dot{V}$ is the volumetric flow rate, and V_c the calciner volume. Moreover, $\dot{V}$ is the product of the gas velocity multiplied by the cross-sectional area of the reactor, which in the study case must be corrected by subtracting the area occupied by the solid. The variation in the effective cross-sectional area along the reactor may be neglected as $CaCO_3$ is consumed when CaO is produced.

Besides, it is assumed that the pressure inside the reactor remains constant. Hence, the volumetric flow rate is given by (9), according to the ideal gas law:

$$\dot{V}_{L2} = \frac{(1 + X_{L2}) \cdot T_{L2}}{T_{L1}} \dot{V}_{L1} \tag{9}$$

The residence time of the gas, through a length L_i in which $\dot{V}_{Li}$ can be considered constant will be $t_{g(L1)} = L_i \cdot S_{eff}/\dot{V}_{Li}$.

3.4 Heat transfer model

The following steps are taken to compute the heat transfer to the cloud of gas and particles to the cooling fluid. First, an energy balance inside the reactor is computed for each slice of reactor (from length L_{i-1} to length L_i) by (10):

$$\sum_{\substack{j=CaO,\\ CO2,\\ CaCO3}} Cp_j \cdot \dot{n}_{j,L_i} \cdot \left(T_{L_i} - T_{L_{i-1}}\right) = \Delta H_r \cdot \left(\dot{n}_{CaCO3,L_i} - \dot{n}_{CaCO3,L_{i-1}}\right) + \dot{q}'_{L_i} \cdot (L_i - L_{i-1}) \quad (10)$$

where Cp_j and $\dot{n}_{j,}$ are the specific heat and mole flow of component j, respectively, T is the temperature of the cloud of gas and particles (which is assumed homogeneous inside the carbonator), ΔH_r is the heat of reaction (178 kJ/mol), and $\dot{q}'_{L_i}$ is the heat flow throughout the inside wall of the carbonator per unit of length. The latter accounts for radiation and convection, in the form of (11):

$$\dot{q}'_{L_i} = \dot{q}'_{rad,L_i} + \dot{q}'_{conv,L_i} \quad (11)$$

$$\dot{q}'_{rad,L_i} = \frac{\varepsilon_w}{\alpha_{g+p} + \varepsilon_w - \alpha_{g+p} \cdot \varepsilon_w} \cdot \sigma \cdot (\varepsilon_{g+p} \cdot T^4_{iw,L_i} - \alpha_{g+p} \cdot T^4_{L_i}) \cdot 2\pi r \quad (12)$$

$$\dot{q}'_{conv,L_i} = h_{g,L_i} \cdot \left(T_{iw,L_i} - T_{L_i}\right) \cdot 2\pi r \quad (13)$$

where α_{g+p} and ε_{g+p} are the absorptivity and emissivity of the gas-particle mixture, ε_w the emissivity of the carbonator wall, σ is the Boltzmann's constant, T_{iw} is the temperature of the inner wall of the carbonator, r the inner radius of the carbonator, and h_g the convective coefficient.

Besides, the model for the calculation of the convective coefficient is borne out of 'Heat Transfer' by Nellis G and Klein S [23], and follows (14) to (18):

$$h_{g,L_i} = \frac{Nu_{Li} \cdot k_{Li}}{2r} \quad (14)$$

$$Nu_{L_i} = 3.66 + \frac{\left(0.049 + \frac{0.020}{Pr_{Li}}\right) \cdot Gz_{Li}^{1.12}}{1 + 0.065 \cdot Gz_{Li}^{0.7}} \quad (15)$$

$$Pr_{Li} = \frac{Cp_{Li} \cdot \mu_{Li}}{k_{Li}} \quad (16)$$

$$Gz_{Li} = \frac{Re_{Li} \cdot Pr_{Li}}{L/2r} \quad (17)$$

$$Re_{Li} = \frac{4 \cdot \dot{m}_{Li}}{\pi \cdot 2r \cdot \mu_{Li}} \quad (18)$$

where Nu is the Nusselt number, k the thermal conductivity, Pr the Prandtl number, Gz the Graetz number, μ the viscosity, Re the Reynolds number, and $\dot{m}$ the mass flow.

The temperature of the outer wall of the calciner, T_{ow}, is computed by the formula of heat conduction through a tube wall, given by (19):

$$\dot{q}'_{L_i} = \frac{T_{ow,L_i} - T_{iw,L_i}}{R_{tube} \cdot L_i} \quad (19)$$

$$R_{tube} = \frac{\ln(\frac{r_{out}}{r})}{2\pi \cdot k_{tube} \cdot L_i} \quad (20)$$

where R_{tube} (20) is the thermal resistance of the carbonator tube, r_{out} the outer radius of the calciner, and k_{tube} the thermal conductivity of the calciner tube (0.025 kW/m·K).

4. Results

The first step to estimate the heat requirements distribution in the calciner for different temperatures is the simulation of isothermal operation. The heat requirements obtained under this scenario would represent the minimum heat flow demanded to achieve a specific temperature and a given final conversion. Once this heat flow has been estimated, several cases which pretend to be closer to a potential implementation of the multi-stage solar calciner are proposed.

4.1. Isothermal operation

The demand of heat per length unit required to maintain constant temperature in the calciner has been calculated in the simulations. These values will be used to define the heat flow pattern introduced along the calciner and the power. The following cases implement the GRP calcination kinetic model and consider isothermal operation. It is important to notice that EES simulations have been run under 100% CO_2 atmosphere while applied GRP model has been adjusted using experimental data obtained under 20% CO_2 in N_2 atmosphere.

The pressure inside the calciner is assumed 1.0 bar and the simulated temperatures within the reactor vary from 900ºC to 975ºC. The initial mass flowrate of $CaCO_3$ is 5 kg/h. The GRP model provides a more accurate value of conversion profile along the calciner than other models. Thus, it is the most suitable to realistically define the required heat distribution along the calciner, Figure 2.

The calculated residence time of the particles ranges between 28-63 seconds (particle diameter of 60 μm) depending on the temperature (975 ºC-900 ºC) and the corresponding conversion of limestone. The higher conversion, the higher production of CO_2 and the higher velocity of the gas and solid cloud inside the calciner. The equilibrium temperature for a 100% CO_2 atmosphere and atmospheric pressure is aprox. 895ºC.

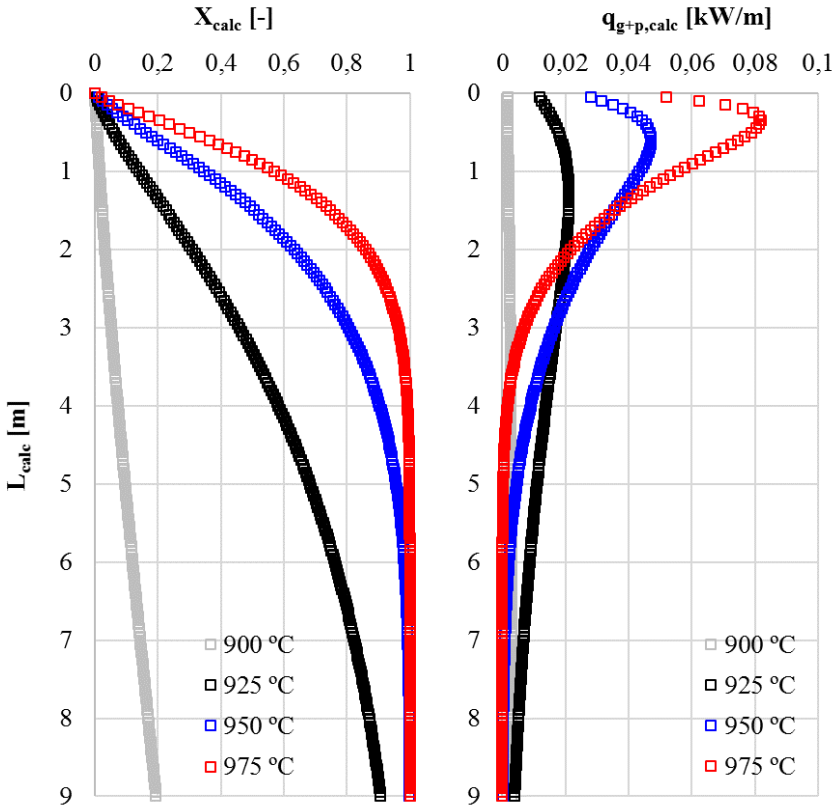

Figure 2. (a) Conversion profiles of the calciner (X) vs. length, (b) required heat per unit length (q) vs. length.

The conversion profiles of the calciner are presented in Figure 2 together with required heat flux per unit length. The final conversion varies from 20% to 100% for 900ºC and 950-975ºC respectively. If temperature is kept between 950-975ºC, total conversion is ensured in the calciner outlet under the simulated conditions. Thus, the maximum storage efficiency is achieved in those cases. Total heat requirement for the cases which achieve complete calcination (100% conversion), 950 and 975 ºC, are 2468 and 2470 W respectively.

It is also observed that the last meters of the calciner are not required since calcination reaction velocity is fast enough to ensure total conversion at lengths lower than 7 m. This heat requirement could correspond to primary solar radiation in the range of 4940 and 8233 W.

4.2. Discretized multi-stage solar reactor

In a single-stage solar calciner, this kind of distribution of heat will not be achieved and the most probable distribution will be a uniform distribution of heat along the whole length, i.e. constant value of kW/m. Thus, a discretization of the reactor must be foreseen and each calciner reactor stage must be designed to receive a different solar input. A first approach of six-stages solar in-series reactors is explored to understand the evolution of needs of heat and assess the efficiency of the system.

4.2.1. Six-stages solar reactor

The next proposal of heat distribution in six different elements with uniform heat fluxes pretends to assess the total heat demand while operating at the lowest possible temperature to achieve total calcination. This case study considers an inlet temperature of the $CaCO_3$ from the solar calciner of 895 ºC. The heat power provided to each reactor which have been simulated are distributed in two 6-stages profiles (a): (i) 1 m 500 W/m, (ii) 1 m 1000 W/m, (iii) 1 m 500 W/m, (iv) 1 m 300 W/m, (v) 2 m 80 W/m, (vi) 1 m 50 W/m, (vii) 2 m without heat input and (b): (i) 1 m 790 W/m, (ii) 1 m 810 W/m, (iii) 1 m 500 W/m, (iv) 1 m 300 W/m, (v) 2 m 80 W/m, (vi) 1 m 10 W/m, (vii) 2 m without heat input.

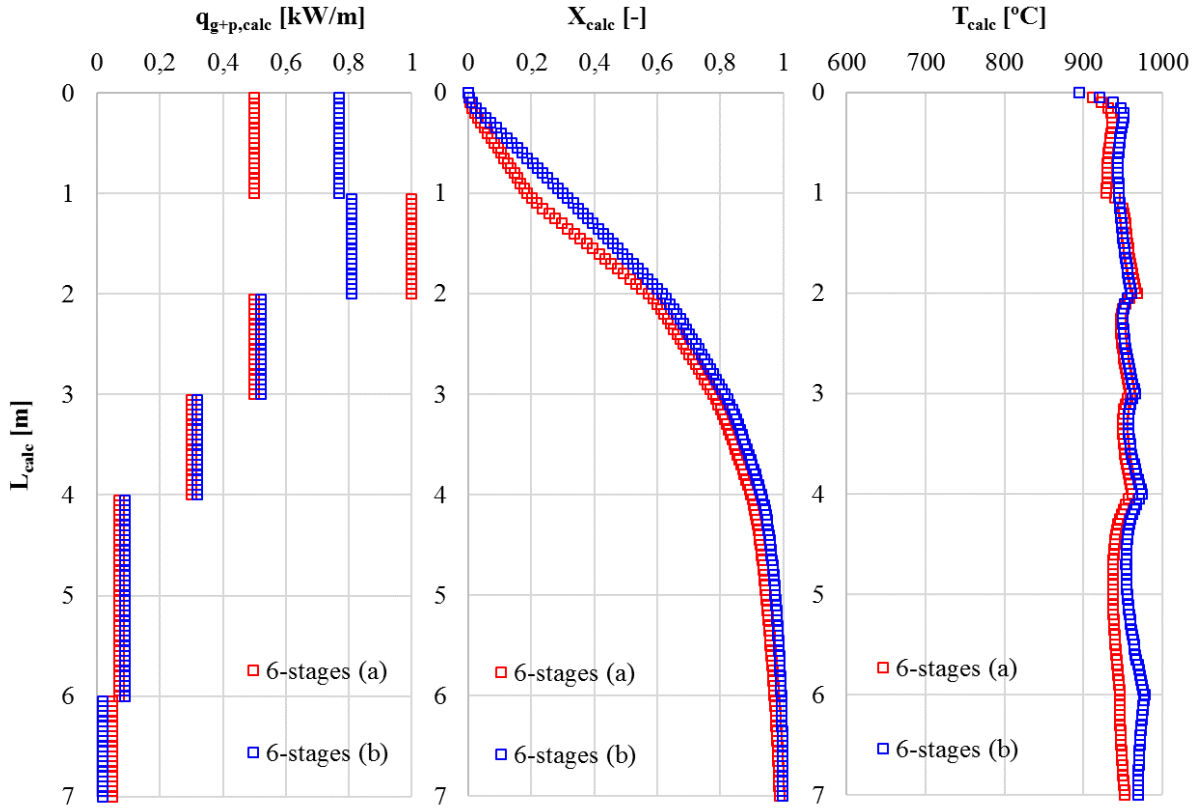

Figure 3. (a) Supplied heat per unit length, (b) Temperature (T) and (c) Conversion profile of the calciner (X) vs. calciner length.

These distributions and the temperature profiles along the calciner are shown in Figure 3 (a). These heat supply distributions achieve the total calcination of limestone (ca. 7.0-7.5 meters) without strong temperature peaks and a flat temperature profile around 950ºC (average temperature 945ºC [6-stages (a)] and 960ºC [6-stages (b)]). The total heat powers provided are 2490 W and 2510 W along the six reactors to achieve a 98,4% and 99,9% of calcination conversion respectively.

Figure 3 presents the comparison between both profiles, profiles 6-stages (a) and 6-stages (b), and shows total calcination for both scenarios. Heat supply and temperatures are somehow lower for profile 6-stages (a) and the consequent slower calcination reaction is illustrated in Figure 3 (b). The thermal energy storage efficiencies for each scenario are 97,6% and 98,3%, respectively.

4.2.2. Three-stages solar reactor

This case assesses the behavior of three-stages solar calciners with heat fluxes of (a) 800, 300 and 30 W/m with a length of 2,25 m and (b) 700, 350 and 30 W/m with a length of 2,25 m. The initial temperature considered for the introduced limestone is 895 ºC. Near total conversion of limestone (99.78% and 97.73% for (a) and (b) respectively) is achieved at the outlet of the calciner as observed in Figure 4 (b). The total requirement of heat for these configurations are 2627 W and 2441 W respectively which could correspond up to 8756 W of primary solar radiation, 6% higher than the minimum requirement (isothermal operation). The thermal energy storage efficiencies for each scenario are 93,81% and 98,9%, respectively.

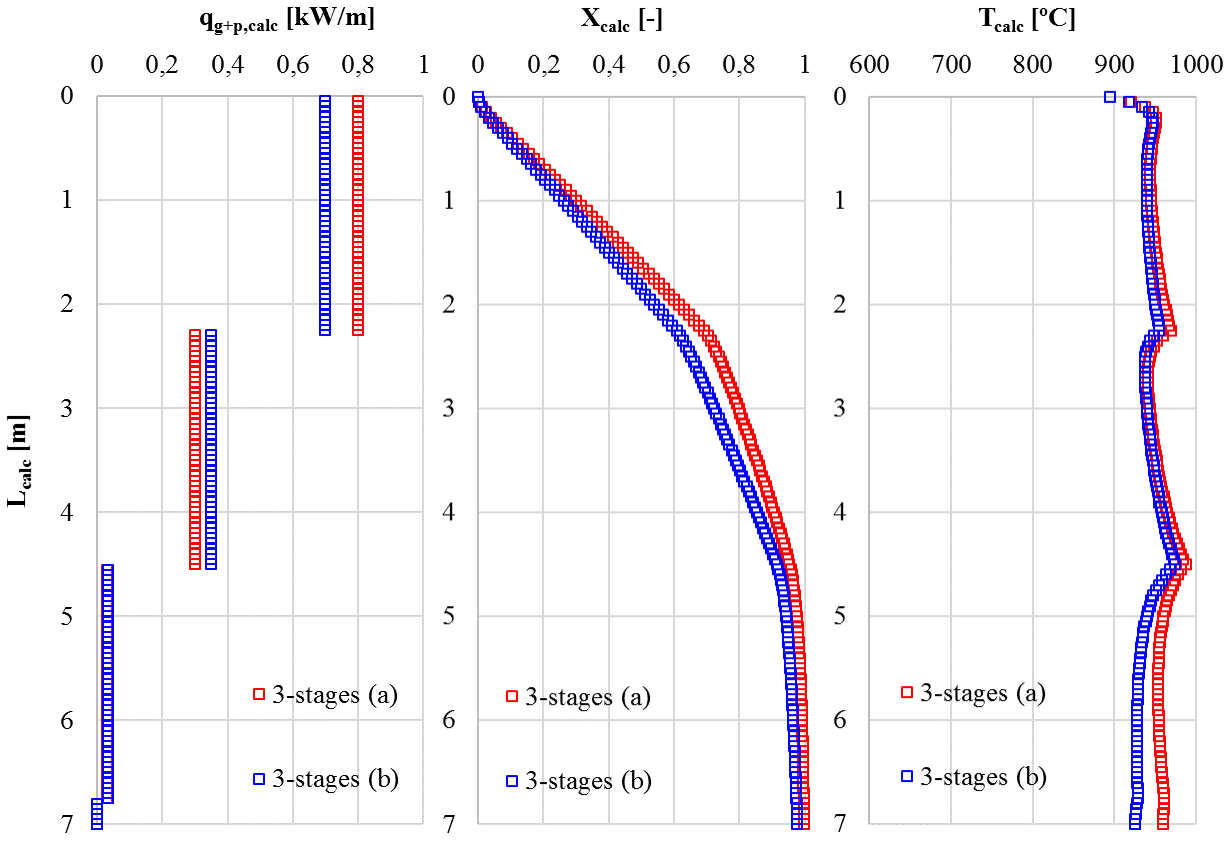

Figure 4. (a) Supplied heat per unit length (q), (b) Temperature (T) and (c) Conversion profile of the calciner (X) vs. calciner length.

5. Conclusions

This paper analyses the behaviour of multi-stage solar calciner reactors under different situations with the target of the highest possible energy storage efficiency and the lowest possible temperatures. The highest possible energy storage efficiency is related to the highest calcination conversion in the

reactor while the lowest possible temperatures are required to limit sintering of lime and to maintain the sorption capacity of the cycled material. It will also be considered the size of the solar calciner since those reactors with fewer stages will present much lower CAPEX. A deeper study of storage efficiency, economic assessment and maximum temperatures much be further developed.

Obtained results show that multi-stage designs which operates at lower heat flow inputs may be more interesting since peak temperature are not present in the profile of temperatures. Although final conversion of limestone is somehow limited in these situations (around 97%), the final efficiency of solar thermal energy storage may even be higher. However, the major advantage of these designs will be related to the milder temperature distribution along the different stages of the calciner reactor.

Acknowledgments

The research leading to these results has received funding from the European Union Horizon 2020 research and innovation programme under grant agreement No 727348, project SOCRATCES.

Nomenclature

Variables:

- b calculation parameter, 1/s
- Cp specific heat, kJ/(kmol·K)
- d diameter, m
- E_a calcination activation energy, kJ/mol
- g gravity, m/s^2
- Gz Graetz number, -
- h convective heat transfer coefficient, kW/(m^2·K)
- k thermal conductivity, kW/(m·K)
- k_0 pre-exponential factor, m/s
- L length, m
- L_{A0} pore surface area, m^2/m^3
- $\dot{m}$ mass flow rate, kg/s
- $\dot{n}$ mole flow rate, kmol/s
- Nu Nusselt number, -
- P pressure, bar
- Pr Prandtl number, -
- $\dot{q}'$ heat flux per unit of length, kW/m
- r reaction front velocity, m/s
- r radius, m
- R thermal resistance, K/kW
- $\mathcal{R}$ ideal gas constant, kJ/(kmol·K)
- S_{A0} pore surface area, m^2/m^3
- S_{eff} effective cross-sectional area of reactor, m^2
- t reacting time or residence time, s
- T temperature, K
- v velocity, m/s
- V volume, m^3
- $\dot{V}$ volumetric flow rate, m^3/s
- X conversion, -
- ΔH_r enthalpy of calcination, kJ/kmol

Greek symbols

- α absorptivity, -
- ε emissivity, -
- θ *GRPM* kinetic parameter, -
- μ viscosity, kg/(m·s)
- ρ density, kg/m^3
- σ Stefan-Boltzmann constant, kW/(m^2·K^4)

Subscripts and superscripts

- c calciner
- $conv$ convection
- eq equilibrium
- g gas
- i initial value or discretization index for axial position

iw	inner wall	rad	radiation
j	component j	s	solid
L	covered length	t	terminal velocity
out	outer radius or diameter	$tube$	calciner tube
ow	outer wall	w	wall
p	particle		

References

[1] D. Kearney, B. Kelly, U. Herrmann, R. Cable, J. Pacheco, R. Mahoney, H. Price, D. Blake, P. Nava, and N. Potrovitza, "Engineering aspects of a molten salt heat transfer fluid in a trough solar field," *Energy*, vol. 29, pp. 861–870, 2004.

[2] S. Kuravi, J. Trahan, D. Y. Goswami, M. M. Rahman, and E. K. Stefanakos, "Thermal energy storage technologies and systems for concentrating solar power plants," 2013.

[3] H. M. Kyaw K, Matsuda H, "Applicability of carbonation/decarbonation reactions to high-temperature thermal energy storage and temperature upgrading.," *J Chem Eng Jpn*, vol. 29, pp. 119–125, 1996.

[4] L. M. Romeo, J. C. Abanades, J. M. Escosa, J. Paño, A. Giménez, A. Sánchez-Biezma, and J. C. Ballesteros, "Oxyfuel carbonation/calcination cycle for low cost CO_2 capture in existing power plants," *Energy Convers. Manag.*, vol. 49, no. 10, 2008.

[5] A. Perejón, L. M. Romeo, Y. Lara, P. Lisbona, A. Martínez, and J. M. Valverde, "The Calcium-Looping technology for CO_2 capture: On the important roles of energy integration and sorbent behavior," *Appl. Energy*, vol. 162, 2016.

[6] P. Lisbona, A. Martínez, Y. Lara, and L. M. Romeo, "Integration of carbonate CO_2 capture cycle and coal-fired power plants. A comparative study for different sorbents," *Energy and Fuels*, vol. 24, no. 1, pp. 728–736, 2010.

[7] R. Chacartegui, A. Alovisio, C. Ortiz, J. M. Valverde, V. Verda, and J. A. Becerra, "Thermochemical energy storage of concentrated solar power by integration of the calcium looping process and a CO_2 power cycle," *Appl. Energy*, vol. 173, pp. 589–605, 2016.

[8] C. Ortiz, R. Chacartegui, J. M. Valverde, A. Alovisio, and J. A. Becerra, "Power cycles integration in concentrated solar power plants with energy storage based on calcium looping," *Energy Convers. Manag.*, vol. 149, pp. 815–829, 2017.

[9] Q. Peng, X. Yang, J. Ding, X. Wei, and J. Yang, "Design of new molten salt thermal energy storage material for solar thermal power plant," *Appl. Energy*, vol. 112, pp. 682–689, 2013.

[10] Q. Peng, J. Ding, X. Wei, J. Yang, and X. Yang, "The preparation and properties of multi-component molten salts," *Appl. Energy*, vol. 87, no. 9, pp. 2812–2817, 2010.

[11] J. Parkkinen, K. Myöhänen, J. Carlos, and B. Arias, "Modelling a calciner with high inlet oxygen concentration for a calcium looping process," *Energy Procedia*, vol. 114, no. November 2016, pp. 242–249, 2017.

[12] I. Martínez, G. Grasa, J. Parkkinen, T. Tynjälä, T. Hyppänen, R. Murillo, and M. C. Romano, "Review and research needs of Ca-Looping systems modelling for post-combustion CO_2 capture applications," *Int. J. Greenh. Gas Control*, vol. 50, pp. 271–304, 2016.

[13] N. Rodriguez, M. Alonso, G. Grasa, and J. C. Abanades, "Heat requirements in a calciner of $CaCO_3$ integrated in a CO_2 capture system using CaO," vol. 138, pp. 148–154, 2008.

[14] L. Luo, K. E. N. Tsoukpoe, H. Liu, and N. Le Pierre, "A review on long-term sorption solar energy storage," vol. 13, pp. 2385–2396, 2009.

[15] N. R. Rhodes, A. Barde, K. Randhir, L. Li, D. W. Hahn, R. Mei, J. F. Klausner, and N.

Auyeung, “Solar Thermochemical Energy Storage Through Carbonation Cycles of $SrCO_3$ / SrO Supported on $SrZrO_3$,” pp. 3793–3798, 2015.

[16] C. Ortiz, R. Chacartegui, J. M. Valverde, and J. A. Becerra, “A new integration model of the calcium looping technology into coal fired power plants for CO_2 capture,” *Appl. Energy*, vol. 169, pp. 408–420, 2016.

[17] S. K. Bhatia and D. D. Perlmutter, “Effect of the product layer on the kinetics of the CO_2-lime reaction,” *AIChE J.*, vol. 29, no. 1, pp. 79–86, Jan. 1983.

[18] G. R. Gavalas, “A random capillary model with application to char gasification at chemically controlled rates,” *AIChE J.*, vol. 26, no. 4, pp. 577–585, Jul. 1980.

[19] R. H. Borgwardt, “Calcination kinetics and surface area of dispersed limestone particles,” *AIChE J.*, vol. 31, no. 1, pp. 103–111, Jan. 1985.

[20] M. Kendall and P. A. P. Moran, *Geometrical probability*. New York: Hafner Pub. Co., 1963.

[21] F. García-Labiano, A. Abad, L. F. de Diego, P. Gayán, and J. Adánez, “Calcination of calcium-based sorbents at pressure in a broad range of CO_2 concentrations,” *Chem. Eng. Sci.*, vol. 57, no. 13, pp. 2381–2393, Jul. 2002.

[22] C. Y. Wen and T. Z. Chaung, “Entrainment Coal Gasification Modeling,” *Ind. Eng. Chem. Process Des. Dev.*, vol. 18, no. 4, pp. 684–695, 1979.

[23] G. Nellis and S. Klein, *Heat transfer*. Cambridge University Press, 2008.